

A Robust Continuation Method to Pass Limit-Point Instability

Kavous Jorabchi,

Mechanical Engineering Department, University of Wisconsin - Madison
2050 Mechanical Engineering Building
1513 University Ave., Madison WI, USA
E-mail: kJORABCHI@WISC.EDU

Krishnan Suresh (Corresponding Author)

Mechanical Engineering Department, University of Wisconsin - Madison
2059 Mechanical Engineering Building
1513 University Ave., Madison WI, USA
Tel: 608-262-3594, Fax: 608-265-2316, E-mail: suresh@ENGR.WISC.EDU

Abstract

In this paper a homotopy map is proposed to pass limit points of snap-through problems encountered in geometrically nonlinear finite element analysis. In the vicinity of such points, the tangent stiffness matrix becomes ill-conditioned, which detrimentally affects the convergence of numerical schemes such as Newton-Raphson method.

The proposed method overcomes this problem by tracing a well-conditioned path instead of the equilibrium path in the vicinity of critical points. This allows the solution procedure to by-pass the critical point without experiencing ill-conditioning. An instance of such a well-conditioned path is constructed for limit points. In particular, starting from the stable (or unstable) configuration, we compute the unstable (or stable) configuration via a robust numerical procedure. Further, since the tangent matrix derivation is consistent with the residual force computation, the quadratic convergence of Newton-Raphson method is retained.

Keywords: Geometric Nonlinearity, Finite Element Analysis, Structural Stability, Snap-through, Limit Points, Ill-conditioning.

1. Introduction

Stability analysis is one of the most important design considerations in structural engineering. Many structures such as bars, beams, plates and shells (which have at least one dimension much smaller than others) can exhibit structural instability under certain loading conditions even when the loads are well below yield point of constituent material. Such behavior is not associated with material failure but rather a significant configurational change of structure. Hence, the problem of elastic instability

inevitably requires use of nonlinear theory of elasticity where one needs to account for geometric nonlinearities and large deformations.

Stability analysis of geometrically nonlinear elastic structures entails obtaining the entire load-displacement path. However, computing the load-displacement path can be challenging due to existence of critical points. Critical points are commonly categorized into bifurcation points and limit points [1] as shown in Figure 1. This figure also illustrates another class of points known as turning points. Turning points are regular points

and have less physical/computational significance [2]. The focus of this paper is on limit points.

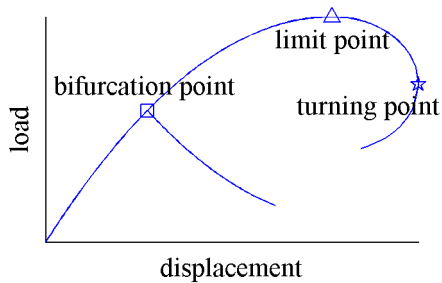


Figure 1, Typical load-displacement graph

In the vicinity of a limit point, the tangent stiffness matrix of finite element formulation becomes ill-conditioned giving rise to two problems: (1) the underlying algebraic system of equations becomes harder to solve using numerical solvers [3, 4], (2) solution jumps to a distant stable configuration making it harder for a numerical method to converge [5]. Numerous techniques, reviewed below, have been proposed to overcome these two problems. We only cover the techniques that are concerned with geometrically nonlinear Finite Element Analysis (FEA).

Bergan [6] proposed to suppress equilibrium iterations until the limit point is passed. This solves both problems; however, the technique unfavorably produces a drift from equilibrium path. An alternative technique was proposed by Wright and Gaylord [7] that entails adding a fictitious spring to stabilize the tangent stiffness matrix in the vicinity of a limit point. However, their approach appears to be unsuitable for general structures.

Argyris [8] proposed a class of methods referred to as displacement control methods. Different variations of these methods are formulated for example in [9, 10]. The method in [10], for instance, preserves symmetry and banded form of tangent stiffness matrix.

Displacement control methods successfully overcome abovementioned problems. However, they fail to trace the equilibrium path beyond a turning point. Moreover these methods implicitly assume that there exists at least one degree of freedom with a monotonic evolution. However, such a degree of freedom may not exist (see for example [11]), and even if it exists, there is no systematic approach to find it.

Thurston et al. [12] proposed a different technique where modal transformation was used to control the behavior of ill-conditioned modes associated with small eigen-values. However, this method requires computation of higher order terms in residual vector in order to make the resulting modal equations consistent; hence the method is computationally expensive.

Clarke et al. [13] summarized yet another class of methods which are obtained by augmenting FEA equations with a constraint equation. Depending upon the type of the constraint equation, many techniques have been derived among which arc-length methods [1, 5, 14-17] have gained popularity over the past years. Further developments in arc-length type methods are summarized in [18-24].

Arc-length methods are well-established and have been widely used in commercial finite element packages. However, as Müller [3, 4] mentioned, these methods suffer from ill-conditioning in the vicinity of critical points in that “*numerical defect of the stiffness matrix is usually not repaired (exception: Wriggers and Simo [25], Felippa [26]). It is commonly assumed that during iteration the critical point is not precisely hit*”. In case of a precise hit, the solution is usually perturbed and the load step is repeated [27]. Riks [16] showed that this shortcoming stems from particular formulation of constraint equation. An alternative formulation was

proposed in [16] that led to a robust algorithm near limit points. However, this technique does not generalize to all constraint equations. Moreover, one needs to employ *linearized* constraint equation at each corrector step (unlike Crisfield’s method [5]). Crisfield et al. [28] reported severe difficulties with conventional cylindrical arc length method and appealed to hybrid static/dynamic procedure to overcome these difficulties. Further failure modes of arc length methods are summarized by Carrera in [29].

For the reasons mentioned above, Belytschko et al. [30] believe that “*tracing of equilibrium branches is often quite difficult; robust and automatic procedures for continuation are not yet available*”. To address these challenges, Müller [3, 4] proposed a stabilized Newton-Raphson method. Stabilization methods are widely used in commercial FEA packages. However, we identify following shortcomings with such techniques:

- 1) Larger number of iterations might be required to jump between two successive, but far apart, stable configurations.
- 2) Quadratic convergence of Newton method is compromised due to inconsistency between the stabilized tangent matrix and residual vector.
- 3) Only the *loading* path is captured as shown in Figure 2. As can be observed in this figure, there exists a stable portion of equilibrium path which is *not* traced during loading, however, this portion will be traced during unloading. Although stabilization methods can be modified to compute the unloading path, this will require additional iterations.
- 4) The topology of the equilibrium path may not be preserved. In other words, stable but disconnected equilibrium paths may merge giving the analyst a wrong conclusion about

structure’s response in practice. Such paths are frequently observed for imperfect systems; see for example [31].

For these reasons, we believe that there are *computational* merits to trace the entire equilibrium path, despite the fact that only stable branches of a system have *practical* significance.

The proposed method in this paper relies on the concept of homotopy [32] (also referred to as continuation) to overcome the abovementioned problems. The main concept behind homotopy methods is as follows: first an “easy” system of equations to which the solution is trivially obtained is set-up; this easy system is then gradually transformed into the original system of nonlinear equations via a control parameter. Homotopy methods have received considerable attention for solving non-linear differential and algebraic equations, see for example [33, 34] and references therein. More recently, these methods have been successfully applied to solve different instability problems. For examples, Fujii et al. [35] used homotopy path in conjunction with local iterations to compute the stability points of structures. Researchers in [36] solved pull-in instability problem of electromechanical systems via homotopy method. A higher order iterative-corrector method based on homotopy transformation was proposed in [37] and applied to geometrically nonlinear problems.

In this paper, we exploit the homotopy concept to arrive at a robust Newton-Raphson technique. In particular, we construct a different (and well-conditioned) path instead of equilibrium path in the vicinity of critical points to bypass these points. An instance of such a path is derived for limit points in Section 3. Through an adaptive framework, we ensure that the tangent matrix along the path is well-conditioned. Consequently, the proposed technique finds the

unstable (or stable) configuration of the system from stable (or unstable) configuration for the fixed load level, essentially *jumping* over the limit point.

The remainder of the paper is organized as follows. We set up general FEA equations in the context of large deformation elasticity in section 2. The proposed method is formally established in Section 3. Adaptive selection of stabilization parameters is discussed in Section 4. Section 5 presents several numerical examples, followed by conclusion and future work in Section 6.

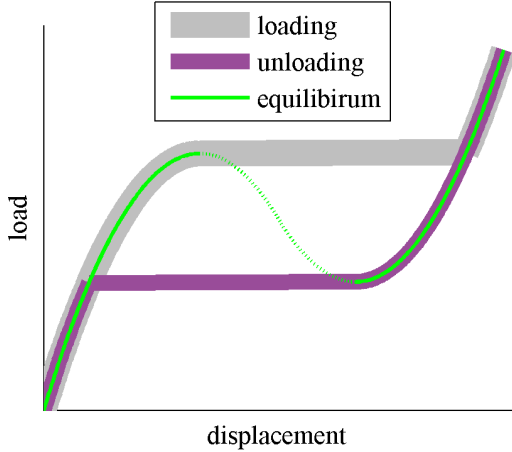


Figure 2, Loading and unloading paths

2. General FEA Equations

Recall that finite element discretization of large displacement elasticity problems results in a system of non-linear algebraic equations of the form [38]

$$\Psi(\mathbf{u}, \lambda) = \mathbf{F}_{\text{int}}(\mathbf{u}) - \lambda \mathbf{F}_{\text{ext}} = \mathbf{0} \quad (2.1)$$

where Ψ is the residual vector, $\mathbf{F}_{\text{int}}(\mathbf{u})$ is the internal force vector which is a nonlinear function of displacement \mathbf{u} , and \mathbf{F}_{ext} is the normalized external load vector which is assumed to be independent of \mathbf{u} . The magnitude of the external load is controlled by λ that is varied as the equilibrium path is traced. The standard Newton-

Raphson scheme is obtained via Taylor-expansion of Equation (2.1)

$$\mathbf{T} \cdot \Delta \mathbf{u} = -\Psi \quad (2.2)$$

where \mathbf{T} is the tangent stiffness matrix defined as

$$\mathbf{T} = \frac{\partial \Psi}{\partial \mathbf{u}} = \frac{\partial \mathbf{F}_{\text{int}}}{\partial \mathbf{u}} \quad (2.3)$$

As mentioned before, matrix \mathbf{T} becomes ill-conditioned in the vicinity of critical points. In the following section, we introduce the proposed method.

3. Derivation of the Proposed Method

As mentioned earlier, the critical points are categorized into bifurcation points and limit points. Only limit points are considered in this paper. A limit point splits the equilibrium path into two portions known as stable and unstable portions. This is shown in Figure 3 which depicts the relation between force intensity λ versus a characteristic displacement u_c . The limit point is encountered when the force magnitude reaches a critical value λ_c . We propose here a methodology to ‘jump’ from point Q1 on the stable portion to the point Q2 on the unstable portion (as opposed to Q3) for a fixed load intensity $\lambda_0 < \lambda_c$. It is assumed that nodal degrees of freedom associated with point Q1, namely \mathbf{u}_0 , are computed via traditional incremental-iterative approach.

The first step in the proposed method is to shift point Q1 to the origin and rewrite Equation (2.1) as

$$\bar{\Psi}(\Delta \mathbf{u}, \Delta \lambda) = \Psi(\mathbf{u}_0 + \Delta \mathbf{u}, \lambda_0 + \Delta \lambda) = \mathbf{0} \quad (3.1)$$

where $\Delta \mathbf{u}$ and $\Delta \lambda$ are respectively increments of solution and force intensity measured from point Q1. The plot of $\Delta \lambda$ as a function of characteristic solution increment Δu_c is shown in Figure 4. As stated above, the objective is to solve Equation (3.1) from Q1 to Q2 for a fixed load intensity, i.e. $\Delta \lambda = 0$. This renders equation (3.1) to

$$\bar{\Psi}(\Delta \mathbf{u}, 0) = \mathbf{0} \quad (3.2)$$

To overcome ill-conditioning of the tangent stiffness matrix, we propose the path defined by the following homotopy map as a replacement for equation (3.2)

$$\mathbf{R}(\Delta \mathbf{u}, p) = (1-p)\mathbf{K} \cdot \Delta \mathbf{u} + \bar{\Psi}(\Delta \mathbf{u}, 0) + p(1-p)\bar{\mathbf{g}} = \mathbf{0} \quad (3.3)$$

where p is the homotopy parameter, \mathbf{K} is a stabilizer matrix and $\bar{\mathbf{g}}$ is ‘‘pseudo load’’ vector; the significance of these two quantities is described below. Note that in Equation (3.3) when $p = 0$, we obtain $\Delta \mathbf{u} = \mathbf{0}$ and when $p = 1$, we recover the original system in Equation (3.2). The stabilizer matrix and pseudo load vector are yet to be determined such that the zero path associated with Equation (3.3) is critical-point-free; this is addressed in Section 4.

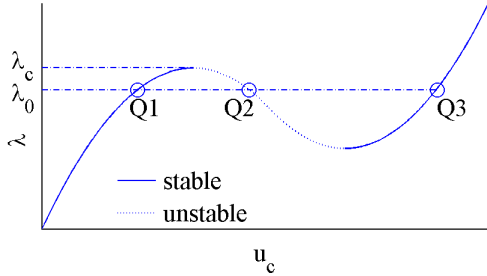


Figure 3, A system with two limit points

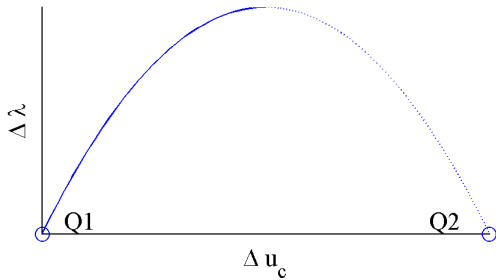


Figure 4, Shifted system

Since we will be relying on classic incremental-iterative scheme for solving Equation (3.3), we rewrite this equation in differential form

$$\begin{aligned} \mathbf{R}(\Delta \mathbf{u} + \delta \Delta \mathbf{u}, p + \delta p) = & \\ (1-p-\delta p)\mathbf{K} \cdot (\Delta \mathbf{u} + \delta \Delta \mathbf{u}) + & \\ \bar{\Psi}(\Delta \mathbf{u} + \delta \Delta \mathbf{u}, 0) + & \\ (p+\delta p)(1-p-\delta p)\bar{\mathbf{g}} = \mathbf{0} & \end{aligned} \quad (3.4)$$

where $\delta \Delta \mathbf{u}$ and δp are increments associated with $\Delta \mathbf{u}$ and p respectively. After linearization and algebraic simplification, above equation reads as

$$\begin{aligned} \mathbf{R}(\Delta \mathbf{u} + \delta \Delta \mathbf{u}, p + \delta p) = \mathbf{R}(\Delta \mathbf{u}, p) + & \\ [(1-p)\mathbf{K} + \mathbf{T}] \cdot \delta \Delta \mathbf{u} + & \\ [-\mathbf{K} \cdot \Delta \mathbf{u} + (1-2p)\bar{\mathbf{g}}] \delta p = \mathbf{0} & \end{aligned} \quad (3.5)$$

where \mathbf{T} is the usual tangent stiffness matrix defined in Equation (2.3). Let \mathbf{S} be the tangent matrix associated with Equation (3.3) i.e. the coefficient matrix for $\delta \Delta \mathbf{u}$ in Equation (3.5)

$$\mathbf{S} = (1-p)\mathbf{K} + \mathbf{T} \quad (3.6)$$

The *incremental step* for the system defined in Equation (3.3) is obtained by substituting $\mathbf{R}(\Delta \mathbf{u}, p) = \mathbf{0}$ in Equation (3.5)

$$\delta \Delta \mathbf{u} = -\mathbf{S}^{-1} \cdot [-\mathbf{K} \cdot \Delta \mathbf{u} + (1-2p)\bar{\mathbf{g}}] \delta p \quad (3.7)$$

and the *iterative step* at a fixed homotopy parameter is obtained by substituting $\delta p = 0$ in Equation (3.5)

$$\delta \Delta \mathbf{u} = -\mathbf{S}^{-1} \cdot \mathbf{R}(\Delta \mathbf{u}, p) \quad (3.8)$$

Observe that both steps in Equations (3.7) and (3.8) require inversion of matrix \mathbf{S} instead of matrix \mathbf{T} . Hence, the homotopy method proposed in Equation (3.3) repairs numerical defect of \mathbf{T} with matrix \mathbf{K} as shown in Equation (3.6). This is mathematically proven for a scalar quadratic equation in below.

Consider a quadratic scalar form for $\bar{\Psi}(\Delta u, \lambda)$ in Equation (3.1)

$$\bar{\psi}(\Delta u, \lambda) = -\Delta u^2 + b\Delta u - \lambda \quad (3.9)$$

where b is a positive scalar. The objective is to start from the trivial solution of equation $(\Delta u, \lambda) = (0, 0)$ and reach the other non-trivial solution $(\Delta u, \lambda) = (b, 0)$ via the proposed method.

Application of Equation (3.3) in Equation (3.9) yields

$$R(\Delta u, p) = (1-p)K \cdot \Delta u - \Delta u^2 + b\Delta u + p(1-p)\bar{g} = 0 \quad (3.10)$$

We now state a lemma which shows that, for the special case of a quadratic equation, the zero path of Equation (3.10) is free of critical points.

Lemma: If $K = -2b$ and $\bar{g} = b^2$ in Equation (3.10) the resulting zero path is linear and hence free of any critical point.

Proof: Solving the quadratic Equation (3.10) for p yields two solutions for p in terms of Δu . Only one of these solutions satisfies the initial condition of $(\Delta u, p) = (0, 0)$, and that is

$$p = \frac{-K\Delta u + \bar{g} - \sqrt{\Delta}}{2\bar{g}} \quad (3.11)$$

where Δ is the discriminant of the quadratic equation

$$\Delta = (K^2 - 4\bar{g})\Delta u^2 + (2K\bar{g} + 4\bar{g}b)\Delta u + \bar{g}^2 \quad (3.12)$$

If we let $K = -2b$ and $\bar{g} = b^2$, Equation (3.11) simplifies to $p = \frac{\Delta u}{b}$ which is a linear relation

between homotopy parameter and solution increment. Hence the corresponding zero path will be critical-point-free proving the lemma. Moreover, since the path is linear, it can be traced with a single Newton iteration.

End of proof

Although the above proof is valid only for quadratic equations, it is well known that (smooth) nonlinear systems can be locally approximated by quadratic equations; hence the importance of the above lemma. Note that the tangent matrix \mathbf{S} in Equation (3.6) is consistent with Equation (3.5) preserving quadratic convergence of Newton-Raphson method. Moreover, if \mathbf{K} is symmetric (see Section 4.1), \mathbf{S} will be symmetric as well (\mathbf{T} is assumed to be symmetric), easily lending Equations (3.7) and (3.8) to solvers optimized for symmetric systems.

Similar techniques have been used in Damped Newton Methods accompanied by line search, see for example [39], and in fictitious penalty spring method [26] and in other stabilization methods [3, 4]. However, unlike these methods, the particular construction of the proposed continuation method in this paper allows iterations to converge to an unstable configuration without experiencing ill-conditioning as will be shown by several examples in Section 5. In the next section, we show how to judiciously select \mathbf{K} and \bar{g} in Equation (3.3) for general nonlinear systems such that the tangent matrix \mathbf{S} does not suffer from ill-conditioning.

4. Stabilization of the Proposed Method

To stabilize the proposed method, an adaptive algorithm is proposed for selecting \mathbf{K} and \bar{g} which is based on the following property of limit points. Here we only consider discrete limit points [1, 40].

Before a limit point is reached (point Q1 in Figure 3), matrix \mathbf{T} is positive definite i.e. all its eigen-values are positive; however past a limit point, one of the eigen-values of matrix \mathbf{T} (usually the smallest eigen-value) becomes negative. In fact, this behavior and a closely related indicator namely determinant of tangent matrix are used by many authors to detect critical points, see for example [1, 18, 41]. For matrix \mathbf{S} to be stable along the solution procedure, this behavior should be eliminated. In other words, none of the eigen-values of \mathbf{S} should change sign during solution procedure.

Note that for $p = 1$ Equation (3.6) yields $\mathbf{S} = \mathbf{T}$, i.e. one of the eigen-values of \mathbf{S} is negative at the end of the path. As stated above, for \mathbf{S} to be non-singular in the solution process, it must retain this characteristic along the solution path, i.e. one the eigen-values of \mathbf{S} (and always

the same one) should be negative. An adaptive selection is employed for the stabilizer matrix \mathbf{K} to meet this requirement. This adaptive method starts with an initial \mathbf{K} and updates it as necessary. Every time \mathbf{K} is updated, \bar{g} must be updated too as explained below. The adaptive method along with initial selection of \mathbf{K} and \bar{g} is discussed next.

4.1 Initial Selection of \mathbf{K} and \bar{g}

At $p = 0$ (point Q1 in Figure 4) all the eigen-values of \mathbf{T} are positive. If the solution is sufficiently close to a limit point, it is safe to assume that the smallest (magnitude wise) eigen-value d will change sign past the limit point. Therefore, the initial \mathbf{K} is formulated as

$$\mathbf{K} = -\alpha d \mathbf{v}^T \cdot \mathbf{v} \quad (4.1)$$

where $\alpha > 1$ is a positive scalar and \mathbf{v} is the eigen-vector associated with eigen-value d . This type of formulation is widely used in stabilization methods to repair numerical defect of tangent matrix by shifting its ill-conditioned modes. Equation (4.1) produces the same eigen-vectors for \mathbf{S} as those of \mathbf{T} which can be easily verified by spectral decomposition [42]. Moreover, the eigen-value of \mathbf{S} associated with \mathbf{v} becomes $(1 - \alpha)d$ which is a negative value (the rest of the eigen-values remain unchanged and hence positive). Although we have considered here only discrete critical points, the form of stabilization used in Equation (4.1) lends itself easily for handling coincident (or closely spaced) critical points as discussed by several researchers (see for instance [4]). However, evaluating eigen-values/vectors can be computationally costly. Müller [3, 4] used Jacobi transformation to compute eigen-values/vectors. Thurston et al. addressed the computation cost associated with computing smallest eigen-value/vector in more details in [12].

Pseudo load \bar{g} is initialized as

$$\bar{g} = \beta \mathbf{F}_{ext} \quad (4.2)$$

where β is a positive scalar; and \mathbf{F}_{ext} , as defined before, is the normalized external force vector.

4.2 Adaptive Algorithm for Updating \mathbf{K} and \bar{g}

Initial selection of \mathbf{K} is guaranteed to produce a stable \mathbf{S} for the first increment. However, \mathbf{S} may loose its desirable characteristic in subsequent iterations. Hence, \mathbf{K} may need to be updated to stabilize the method. Such an update could be similar to Equation (4.1) where d and \mathbf{v} are computed from the most recent tangent stiffness matrix. An alternate method, similar to Equation 15 in [4], is obtained by increasing parameter α in Equation (4.1)

$$\alpha^{new} = \gamma \alpha \quad (4.3)$$

where γ is a scalar quantity greater than 1 (we used $\gamma = 1.5$ for all the examples in Section 5). Once α^{new} is computed from Equation (4.3), it is used in Equation (4.1) instead of α to update \mathbf{K} . Observe that in both of update methods described above, matrix \mathbf{S} undergoes a rank 1 update, hence its inverse to be used in subsequent iteration can be easily updated by Sherman-Morrison-Woodbury formula [42] to save computational work.

Note that updating \mathbf{K} is equivalent to switching from the current solution path (which is found to be ill-conditioned) to a potentially well-conditioned one. This switch is performed at the last converged solution $(\Delta \mathbf{u}, p)$. To form a continuous path between the old and new paths at the last known converged solution $(\Delta \mathbf{u}, p)$, \bar{g} must be updated as well to compensate for changes in \mathbf{K} . If we note changes in \mathbf{K} and \bar{g} by $d\mathbf{K}$ and $d\bar{g}$ respectively, equation (3.3) reads

$$(1-p)\mathbf{K} \cdot \Delta \mathbf{u} + \bar{\mathbf{F}}(\Delta \mathbf{u}, 0) + p(1-p)\bar{\mathbf{g}} =$$

$$(1-p)(\mathbf{K} + d\mathbf{K}) \cdot \Delta \mathbf{u} + \bar{\mathbf{F}}(\Delta \mathbf{u}, 0) + p(1-p)(\bar{\mathbf{g}} + d\bar{\mathbf{g}}) \quad (4.4)$$

which yields

$$d\bar{\mathbf{g}} = \frac{1}{p} d\mathbf{K} \cdot \Delta \mathbf{u} \quad (4.5)$$

For $p = 0$ one can skip the update in Equation (4.5) since Equation (3.3) will be identically satisfied with any $d\mathbf{K}$ because $\Delta \mathbf{u}$ is $\mathbf{0}$.

The proposed algorithm, outlined in Figure 5, can be seen as a combination of three techniques, (1) the stabilization techniques, see for example [3, 4, 26], (2) the correction load technique, see for example [4, 7], and (3) homotopy technique which relies on using a different path other than equilibrium path, introduced in this paper. The algorithm described above is to pass concave limit points (see Figure 4). For convex limit

points, one must use a negative value for β in Equation (4.2).

The entire equilibrium path is traced in the following fashion. Traditional incremental-iterative methods are employed to trace the path from a reference configuration till a limit point. A limit point can be detected by checking the condition number of tangent stiffness matrix or other measures such as “current stiffness parameter” [6]. Once a limit point is reached, the algorithm in Figure 5 is exploited to pass the limit point. After passing the limit point, the remaining portion of equilibrium path is traced till the next limit point is experienced. Note that the portions of the equilibrium path between stable and unstable configurations can not be obtained via the proposed method since a different path was traced to “bridge” these configurations.

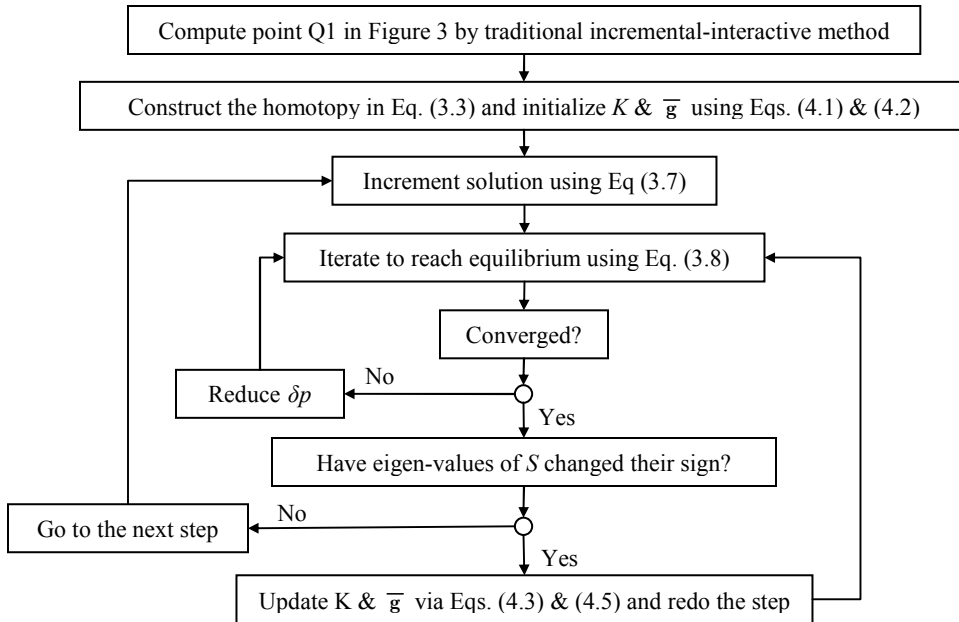


Figure 5, Flow chart of the proposed algorithm.

5. Numerical Experiments

In this section, the proposed method is tested for several snap-through examples. For all of the

examples in this section, $\alpha = 1.5, \beta = 0.1$ & $\gamma = 1.5$ was used. These parameters are selected such that the matrix \mathbf{S} and pseudo load $\bar{\mathbf{g}}$ have similar

scaling as their counterparts i.e. T and F_{ext} respectively. Homotopy parameter p is initially set to 0.1. If convergence is not achieved within the maximum number of iterations, δp is halved. On the other hand, δp is increased by the method proposed in [5] in case of convergence.

The validity of the solutions is verified via *Ansys* [43]. Large deformation flag was activated in *Ansys* to allow for geometric nonlinearities. Arc length method was used with default settings (unless stated otherwise) to allow *Ansys* solver to pass limit points. In all of the experiments the mesh used in *Ansys* was identical to the mesh we used in our method. Moreover, *Ansys* models were analyzed using *Link1* element [43] for trusses and *beam3* element [43] for beams.

5.1 Two Symmetric Three Hinged Trusses

This experiment consists of four link elements showing a pronounced snap-back behavior. The geometry, material property and boundary conditions are shown in Figure 6. Point N is constrained to vertical movement only to prevent the structure from bifurcation.

The default setting of *Ansys* arc length method did not result in convergence for this example, therefore the “maximum multiplier of the reference arc-length radius” was reduced to 3 in order to obtain convergence. The equilibrium path obtained from *Ansys* is shown in Figure 7. The bars in this figure represent number of required equilibrium iterations for each load step. These numbers are normalized to 2 (to increase the clarity of the illustration). As can be readily seen from Figure 7, for arc length method, the number of iterations increases in the vicinity of critical points. Figure 8 shows the path obtained via the proposed method. The number of iterations required to pass each limit point labeled in Figure 8 is listed in Table 1.

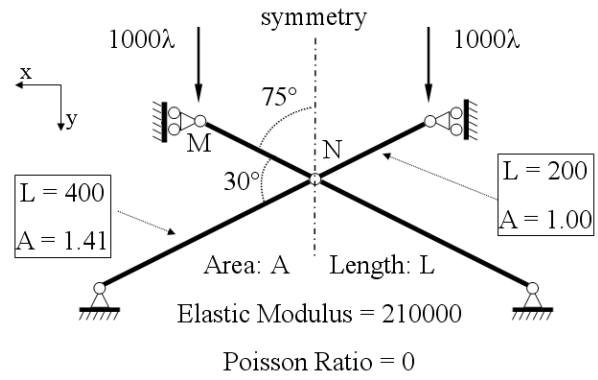


Figure 6, Two symmetric three hinged trusses

Table 1, Number of iterations required for each limit point

Limit point	a	b	c	d	e	f	g	h
# of iterations	13	18	17	14	28	16	18	18

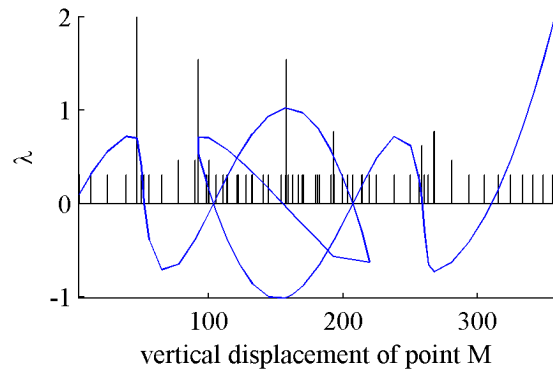


Figure 7, Equilibrium path for experiment 1 obtained via *Ansys*

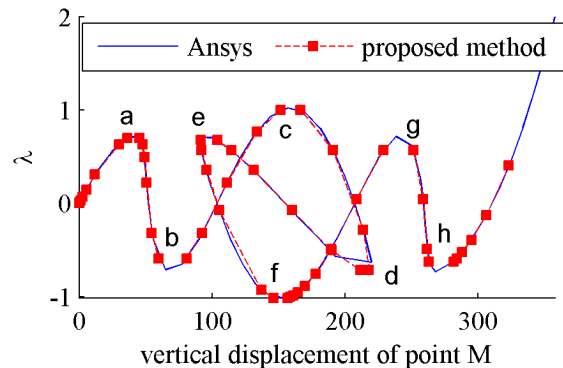


Figure 8, Equilibrium path obtained via proposed method compared to *Ansys*

In order to show that the zero paths taken to pass limit points do not suffer from ill-conditioning, we plot these paths in Figure 9 for each limit point labeled in Figure 8. As can be easily seen from these plots, there are no singularities in the zero paths; hence traditional continuation methods can be readily exploited to trace these paths and thereby *bypass* the limit points. However, such one dimensional plots can be misleading as Bergan et al. [6] emphasized and one needs to observe the behavior of all degrees as freedom to conclude the well-conditionedness of a numerical method. For this example, we plot in Figure 10 the zero paths associated with the

other degree of freedom i.e. vertical displacement of point N (see Figure 6). Figure 9 and Figure 10 together show that the proposed method does not suffer from ill-conditioning. Observe that the zero paths associated with limit points “a, b, d, e, g and h” exhibit turning points; turning points do not pose computational challenge (except for displacement control methods) and hence have no computational significance [2]. Note that plotting all zero paths (Figure 9 and Figure 10) was possible for this example because there existed only two degrees of freedom. For the remaining experiments we will only plot a representative one dimensional graph.

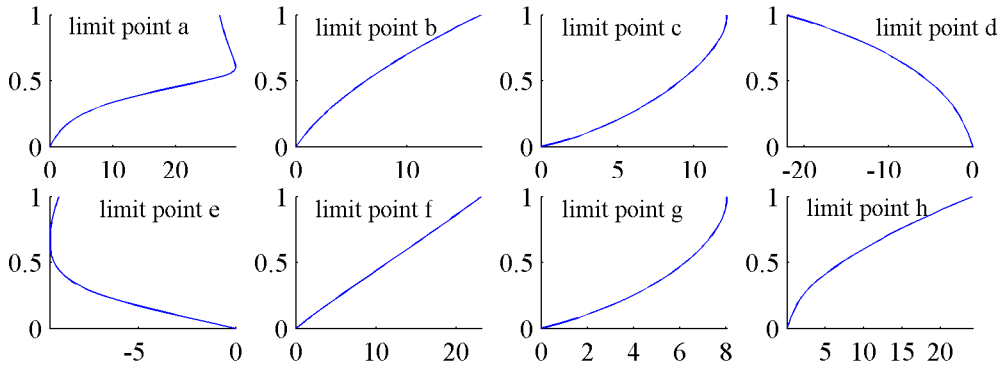


Figure 9, Zero paths. The horizontal axes show the vertical displacement increment of point M (Figure 6), and the vertical axes show the homotopy parameter p (Equation (3.3))

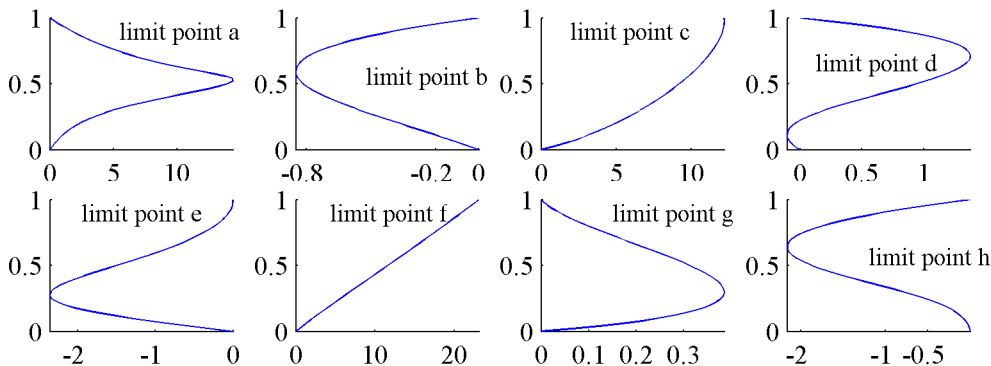


Figure 10, Zero paths. The horizontal axes show the vertical displacement increment of point N (Figure 6), and the vertical axes show the homotopy parameter p (Equation (3.3))

5.2 Frame from Lee et al. [44]

The geometry, material property and boundary conditions of the frame are shown in Figure 11. The frame is modeled with a total of 20 beam elements. The equilibrium path i.e. vertical displacement of point S in Figure 11 versus λ , is obtained using *Ansys* and is shown in Figure 12. The bars represent number of equilibrium iterations required to reach each equilibrium configuration. These numbers are normalized to 1 (to increase the clarity of the illustration). Again, an increased number of iteration is observed near limit points. The equilibrium path obtained via the proposed method is shown in Figure 13. Moreover, the zero paths taken to bypass limit points are plotted in Figure 14 and Figure 15. As can be observed from these figures, the paths are free of any singularity and ill-conditioning and hence can be traced efficiently.

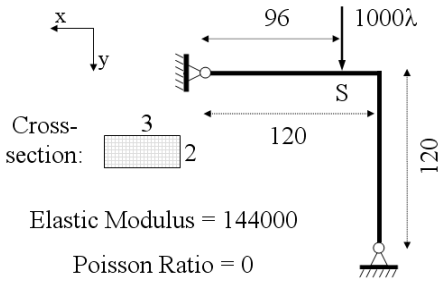


Figure 11, Frame from Lee et al.

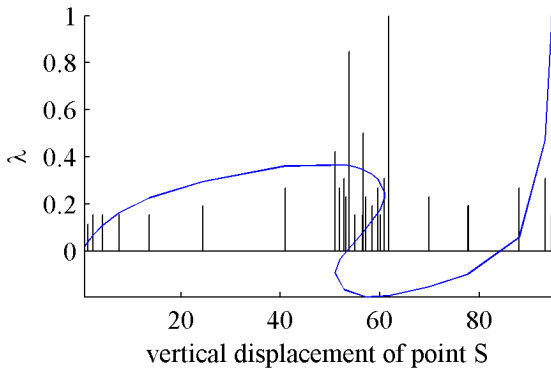


Figure 12, Equilibrium path for experiment 2 obtained via *Ansys*

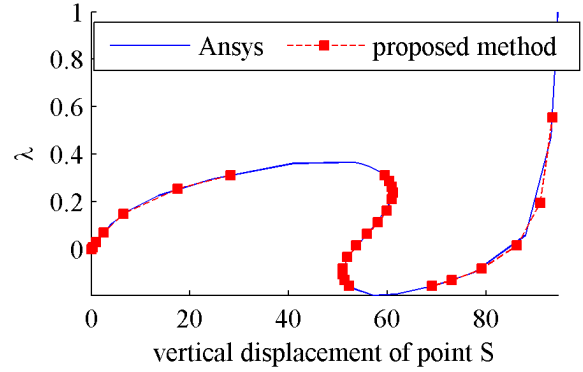


Figure 13, Equilibrium path obtained via proposed method compared to *Ansys*

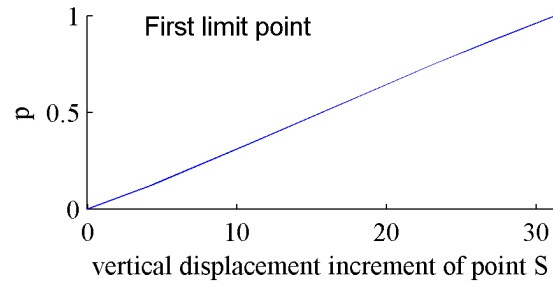


Figure 14, Zero path of the 1st limit point

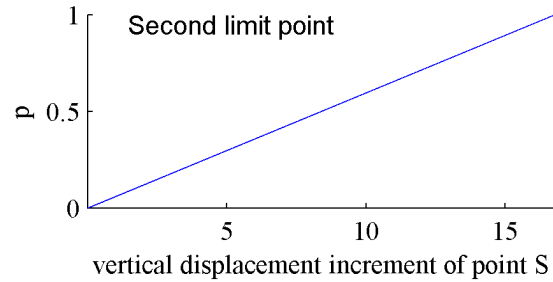


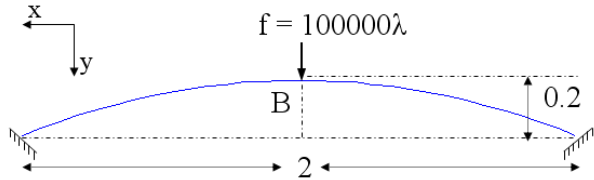
Figure 15, Zero path of the 2nd limit point

5.3 Shallow Arch

This experiment targets snap-through behavior of shallow arch. Two different modeling approaches are tested to show the versatility of the proposed method. In the first approach, 1-D beam elements are exploited to model the shallow arch. In the second approach, the arch is modeled as a 2-D plane stress problem.

The first approach, similar to the previous examples, uses co-rotational formulation [45] to account for large deformations of 1-D beam elements. The geometry, material property and

boundary conditions are shown in Figure 16. The arch is modeled with a total of 30 beam elements. The equilibrium path i.e. vertical displacement of point B versus λ (Figure 16) is obtained using *Ansys* and is shown in Figure 17. The bars represent number of equilibrium iterations required to reach each equilibrium configuration. These numbers are normalized to 1 (to increase the clarity of the illustration). Again, an increased number of iteration is observed at the vicinity of limit points. The equilibrium path obtained via the proposed method is shown in Figure 18. Moreover, the zero paths taken to jump over limit points are plotted in Figure 19 and Figure 20. As can be observed from these figures, the paths are free of any singularity and ill-conditioning and hence can be traced efficiently.



Elastic Modulus = $2e11$, Poisson Ratio = 0
Figure 16, 1D beam model of shallow arch

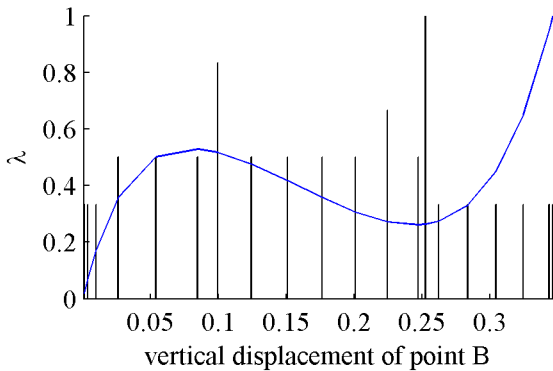


Figure 17, Equilibrium path for shallow arch obtained via *Ansys*

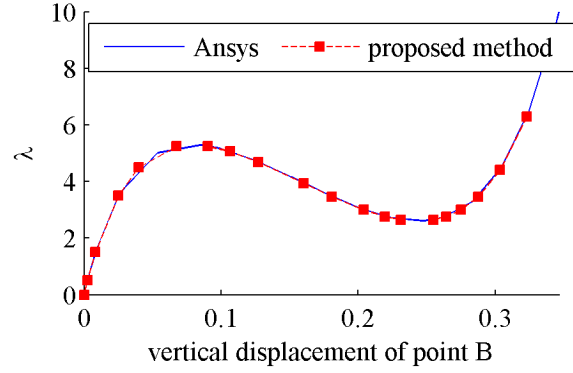


Figure 18, Equilibrium path obtained via proposed method compared to *Ansys*

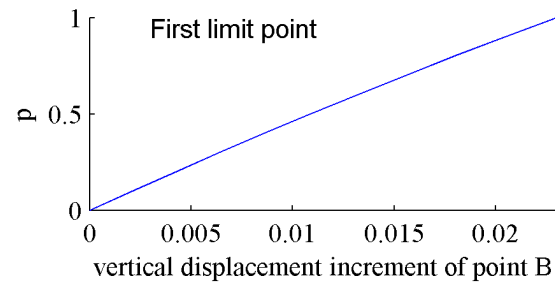


Figure 19, Zero path of the 1st limit point

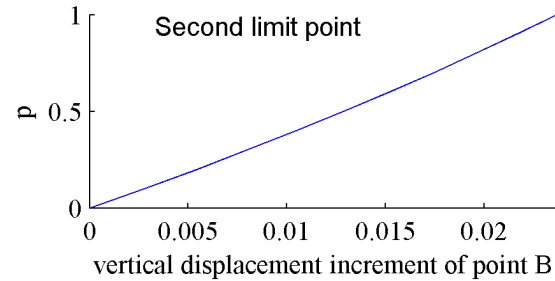


Figure 20, Zero path of the 2nd limit point

The second approach uses 2D plane stress to mode the arch. Total Lagrangian formulation is employed in this model with the following constitutive equation

$$\frac{\partial W(\mathbf{E})}{\partial \mathbf{E}} = \begin{bmatrix} nE_{11} & mE_{12} \\ mE_{12} & nE_{22} \end{bmatrix} \quad (5.1)$$

where W is the internal energy function and \mathbf{E} is Green-Lagrange strain tensor. Here we used $n = 200 \text{ GPa}$ and $m = 100 \text{ GPa}$. The geometry, mesh and the boundary conditions are shown in

Figure 21. The force is applied as a distributed load with a local support of $10^{-110x} \lambda$ where λ is the intensity of the load. *Ansys* was not used in this experiment since exact material model and loading condition used in our code could not be duplicated in *Ansys*.

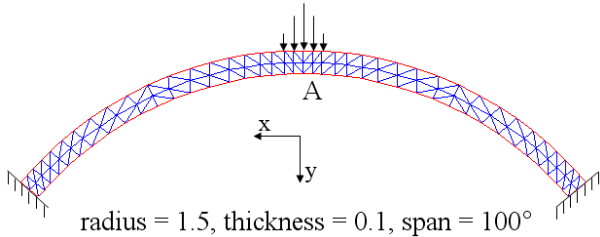


Figure 21, Plane stress model of shallow arch

The proposed homotopy method is successfully applied to this problem. The load-displacement graph i.e. the graph of λ as a function of vertical displacement of point A (see Figure 21) is shown in Figure 22. Missing portions are due to the fact that a different path was traced to jump over the limit points as mentioned before (these gaps exist in previous plots as well).

The path used to jump over the first limit point is shown in Figure 23. As can be seen from this figure, the zero path is critical-point-free and hence can be traced without any difficulty; same holds for the zero path corresponding to the second limit point which is not shown here due to

space limits. The deformed arches corresponding to configurations 1, 2 and 3 (see Figure 22) are shown in Figure 24.

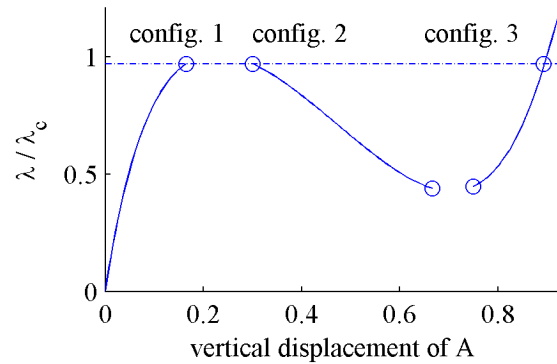


Figure 22, Equilibrium path for 2D plane stress model of shallow arch

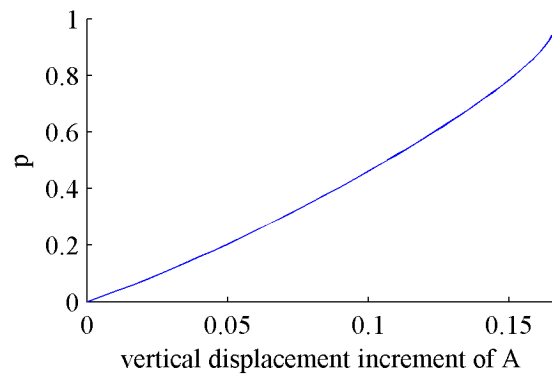


Figure 23, Zero path for the first limit point in Figure 22

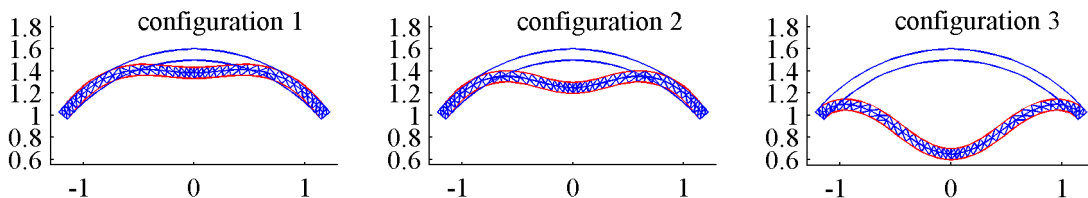


Figure 24, Deformed configurations of the shallow arch

6. Conclusion

A homotopy map was proposed to assist incremental-iterative methods to pass limit points. It was shown that the tangent matrix associated with the method is well-conditioned along the solution path which was achieved via an adaptive algorithm. Numerical experiments illustrated that if the starting point is sufficiently close to a limit point (thereby justifying quadratic form for the nonlinear system), the initial selection of stabilization parameters will be effective throughout the solution process. On the other hand, a farther starting point may require updating stabilization parameters.

Future work will address the following challenges. Since the method “jumps” over limit points, the equilibrium path between the initial and final configurations is missing (for example the maximum load that the structure can tolerate before snapping can not be computed via the proposed method). Further, prior knowledge of snap-through behavior is assumed here. In other words, if the equilibrium path exhibits a flat portion without undergoing snap-through, the proposed method will show a slow convergence or fail to converge to a solution. Moreover, existence of a continuous zero path for the proposed homotopy map remains to be proven. Finally, the extension of the proposed method to pass bifurcation points and multiple limit-bifurcation points is currently being investigation.

Acknowledgment

The authors wish to acknowledge the support of the National Science Foundation under grants OCI-0636206, and CMMI-0726635, CMMI-0745398.

References

1. Riks, E., The application of Newton's method to the problem of elastic stability, *Journal of Applied Mechanics*, 1972, 39(4): p. 1060-1065.
2. Felippa, C.A., Lecture notes in nonlinear finite element methods, Chapter 5, page 6, 2010, Department of Aerospace Engineering Sciences, University of Colorado, Boulder, CO.
3. Müller, M., Passing of instability points by applying a stabilized Newton-Raphson scheme to a finite element formulation: Comparison to arc-length method, *Computational Mechanics*, 2007, 40(4): p. 683-705.
4. Müller, M., Postbuckling analysis stabilized by penalty springs and intermediate corrections, *Computational Mechanics*, 2008, 42(5): p. 631-654.
5. Crisfield, M.A., A fast incremental/iterative solution procedure that handles 'snap-through', *Computers and Structures*, 1981, 13(1-3): p. 55-62.
6. Bergan, P.G., Solution techniques for non-linear finite element problems, *International Journal for Numerical Methods in Engineering*, 1978, 12(11): p. 1677-1696.
7. Wright, E.W., Gaylord, E.H., Analysis of unbraced multistory steel rigid frames, *American Society of Civil Engineers Proceedings, Journal of the Structural Division*, 1968, 94(ST5): p. 1143-1163.
8. Argyris, J., Continua and discontinua, in *Opening address to the International Conference on Matrix Methods of Structural Mechanics*, October 26 1965, Dayton, OH, Wright-Patterson U.S. A.F. Base
9. Nemat-Nasser, S., Sharoff, H.D., Numerical analysis of pre- and post-critical response of elastic continua at finite strains, *Computers and Structures*, 1973, 3(5): p. 983-999.
10. Zheng, H., Liu, D.F., Lee, C.F., Tham, L.G., Displacement-controlled method and its applications to material non-linearity, *International Journal for Numerical and Analytical Methods in Geomechanics*, 2005, 29(3): p. 209-226.
11. Lorentz, E., Badel, P., A new path-following constraint for strain-softening finite element simulations, *International Journal for Numerical Methods in Engineering*, 2004, 60(2): p. 499-526.
12. Thurston, G.A., Brogan, F.A., Stehlin, P., Postbuckling analysis using a general-purpose code, *AIAA Journal*, 1986, 24(6): p. 1013-20.
13. Clarke, J.M., Hancock, G.J., A study of incremental-iterative strategies for non-linear analyses, *International Journal for Numerical Methods in Engineering*, 1990, 29(7): p. 1365-1391.
14. Riks, E., An incremental approach to the solution of snapping and buckling problems, *International Journal of Solids and Structures*, 1979, 15(7): p. 529-551.
15. Riks, E., Some computational aspects of the stability analysis of nonlinear structures, *Computer Methods in Applied Mechanics and Engineering*, 1984, 47(3): p. 219-259.

16. Riks, E., On formulations of path-following techniques for structural stability analysis, Ladeveze P, Zienkiewicz OC, editors. *New advances in computational structural mechanics*. Amsterdam, The Netherlands: Elsevier Science Publishers B.V, 1992: p. 65-79.
17. Wempner, G.A., Discrete approximations related to nonlinear theories of solids, *International Journal of Solids and Structures*, 1971, 7(11): p. 1581-1599.
18. Zhao, Q., Tianqi, Y., On the adaptive parameter incremental method for analyzing the snapping problems, *Applied Mathematics and Mechanics* (English Edition), 1995, 16(9): p. 851-858.
19. Ritto-Coorrea, M., Carnotirn, D., On the arc-length and other quadratic control methods: established, less known and new implementation procedures, *Computers and Structures*, 2008, 86(11-12): p. 1353-1368.
20. Hellweg, H.B., Crisfield, M.A., A new arc-length method for handling sharp snap-backs, *Computers and Structures*, 1998, 66(5): p. 705-9.
21. Csebfalvi, A., A Non-linear path-following method for computing the equilibrium curve of structures, *Annals of Operations Research*, 1998, 81: p. 15-24.
22. Wriggers, P., Wagner, W., Miehe, C., A quadratically convergent procedure for the calculation of stability points in finite element analysis, *Computer Methods in Applied Mechanics and Engineering*, 1988, 70(3): p. 329-347.
23. Wriggers, P., Wagner, W., *Nonlinear Computational Mechanics*, Chapter 2, 1991, Berlin, Springer.
24. Krishnamoorthy C.S., Ramesh, G., Dinesh, K.U., Post-buckling analysis of structures by three-parameter constrained solution techniques, *Finite Element in Analysis and Design*, 1996, 22(2): p. 109-142.
25. Wriggers, P., Simo, J.C., A general procedure for the direct computation of turning and bifurcation points, *International Journal for Numerical Methods in Engineering*, 1990, 30(1): p. 155-176.
26. Felippa, C.A., Penalty spring stabilization of singular jacobians, *Journal of Applied Mechanics, Transactions ASME*, 1987, 54(3): p. 728-729.
27. Felippa, C.A., *Lecture notes in nonlinear finite element methods*, Chapter 18, page 8, 2010, Department of Aerospace Engineering Sciences, University of Colorado, Boulder, CO.
28. Crisfield, M.A., Jelenic, G., Mi, Y., Zhong, H.-G., Fan, Z., Some aspects of the non-linear finite element method, *Finite Element in Analysis and Design*, 1997, 27(1): p. 19-70.
29. Carrera, E., A study of arc-length-type methods and their operation failures illustrated by a simple model, *Computers and Structures*, 1994, 50(2): p. 217-229.
30. Belytschko, T., Liu, W.K., Moran, B., *Nonlinear finite elements for continua and structures*, 1st ed, page 358, 2000, John Wiley & Sons Inc.
31. Thompson, J.M.T., Hunt, G.W., *A general theory of elastic stability*, page 20, 1973, John Wiley & Sons Ltd.
32. Watson, L.T., Numerical linear algebra aspects of globally convergent homotopy methods, *SIAM Review*, 1986, 28(4): p. 529-545.
33. He, J.H., Homotopy perturbation technique, *Computer Methods in Applied Mechanics and Engineering*, 1999, 178(3): p. 257-262.
34. Krauskopf, B., Osinga, H.M., Galan-Vioque, J., *Numerical continuation methods for dynamical systems*, 2007, Dordrecht, Netherlands, Springer.
35. Fujii, F., Okazawa, S., Bypass, homotopy path and local iteration to compute the stability point, *Structural Engineering and Mechanics*, 1997, 5(5): p. 577-586.
36. Moghimi Zand, M. Ahmadian, M.T., Application of homotopy analysis method in studying dynamic pull-in instability of microsystems, *Mechanics Research Communications*, 2009, 36(7): p. 851-858.
37. Cadou J.M., Damil, N., Potier-Ferry, M., Braikat, B., Projection techniques to improve high-order iterative correctors, *Finite Element in Analysis and Design*, 2004, 41(3): p. 285-309.
38. Reddy, J.N., *An introduction to nonlinear finite element analysis*, 2004, New York, USA, Oxford University Press.
39. Ortega, J. M., Rheinboldt, W. C., *Iterative solution of nonlinear equations in several variables*, 1970, New York, Academic Press.
40. Huseyin, K., *Nonlinear theory of elastic stability*, 1975, Leyden, Netherlands, Noordhoff international publishing.
41. Dutta, A., White, D.W., Automated solution procedures for negotiating abrupt non-linearities and branch points, *Engineering Computations*, 1997, 14(1): p. 31-56.
42. Nocedal, J., Wright, S.J., *Numerical optimization*, 2nd ed, Springer Series in Operations Research, 2006, New York, Springer Science + Business Media.
43. ANSYS®, <http://www.ansys.com>. Release 11.0.
44. Lee, S.L., Manuel, F.S., Rossow, E.C., Large deflections and stability of elastic frames, *American Society of Civil Engineers Proceedings, Journal of the Structural Division*, 1968, 94(EM2): p. 521-547.
45. Crisfield, M.A., *Non-linear finite element analysis of solids and structures*, 1991, John Wiley and Sons Ltd.